

Mössbauer study of the $Mn_{1-x}Fe_xNiGe$ system ($0.05 \leq x < 1.0$)

V.I. Mitsiuk ^{a,b,*}, V.V. Khovaylo ^b, A.V. Mashirov ^c, T.M. Tkachenka ^d, Z. Surowiec ^e, M. Budzynski ^e

^a Scientific-Practical Materials Research Center of National Academy of Sciences of Belarus, 220072, Minsk, Belarus

^b National University of Science and Technology MISIS, 119049, Moscow, Russia

^c Kotelnikov Institute of Radio-engineering and Electronics, RAS, 125009, Russia

^d Belarusian State Agrarian Technical University, Belarus

^e Institute of Physics, Maria Curie-Sklodowska University, Maria Curie Skłodowska Sq. 1, 20031, Lublin, Poland

ARTICLE INFO

Keywords:

Mössbauer effect
Magnetic measurements
Nickel arsenide type of structure
Hyperfine interactions

ABSTRACT

Magnetic and Mössbauer measurements were performed for $Mn_{1-x}Fe_xNiGe$ solid solutions. The Mössbauer data obtained suggest that the iron atoms at small concentrations $x < 0.20$ prefer to fill trigonal bipyramidal positions substituting the nickel atoms and thus do not participate in magnetic interactions. This is consistent with a decrease of magnetization in the $x < 0.20$ samples, evident from the magnetic measurements data. As the concentration increases above $x > 0.20$ in $Mn_{1-x}Fe_xNiGe$, the iron atoms replace both the nickel atoms in trigonal bipyramidal and the manganese atoms in octahedral positions.

1. Introduction

Persistent interest expressed by many researchers to the half-Heusler alloys based on MnNiGe has been associated with the existence of a wide variety of magnetic phases and the occurrence of structural and magnetostructural phase transitions in these materials. These transitions are accompanied by significant magnetocaloric and magnetostrictive effects [1–7]. On one hand, the possibility of using the magnetocaloric effect and magnetostriction in the fabrication of effective magnetic refrigerators and magnetostrictors makes the $Mn_{1-x}Fe_xNiGe$ system attractive. On the other hand, the features of the mechanism of giant spontaneous magnetostriction accompanying magnetostructural phase transitions in the $Mn_{1-x}Fe_xNiGe$ alloys is fundamental problem in the physics of magnetic phenomena.

The purpose of the work is to study the features of crystal structure and magnetic properties of $Mn_{1-x}Fe_xNiGe$ ($0.05 \leq x \leq 1.00$) solid solutions.

It was shown that the MnFeGe compound crystallizes into a hexagonal structure of the Ni₂In type (space group *P6₃/mmc*) over the entire temperature range [8]. The results of the neutron diffraction investigations of Mn_{0.95}Fe_{1.0}Ge powder demonstrated that the magnetic moments of manganese atoms are antiferromagnetically ordered at temperatures below 240 K, whereas the magnetic moments of iron atoms are ferromagnetically ordered [9]. At the same time, the MnNiGe

compound at room temperature has an orthorhombic structure of the TiNiSi type (space group *Pnma*) [10,11]. Below the Néel temperature ($T_N = 346$ K), this compound is a helical antiferromagnet. At $T = 528$ K, the MnNiGe compound undergoes a first-order displacive phase transition from the low-temperature orthorhombic structure of the TiNiSi type to the high-temperature hexagonal structure of the Ni₂In type. Similar structural transitions are accompanied by a change in the period of the unit cell and are described by a softening of one of the phonon modes [12], which in MnNiGe, as in MnAs [13], can be stimulated by a strong electron–phonon interaction.

In this work, we have investigated the magnetic and Mössbauer properties of $Mn_{1-x}Fe_xNiGe$ solid solutions with the iron concentration range $0.05 \leq x \leq 1.00$ with the purpose to find out the mechanisms of the formation of magnetostructural phases.

2. Experiment

Polycrystalline solid solutions of $Mn_{1-x}Fe_xNiGe$ were synthesized by the solid-phase reactions. Powders of the initial components, taken in appropriate weight ratios, interacted in evacuated quartz ampoules in a single-zone resistance furnace. The mixture was slowly heated to a temperature of 1323 K, annealed for 3 days at a temperature of 1223 K, followed by quenching in ice water.

The powder XRD diffraction patterns were recorded at room

* Corresponding author. Scientific-Practical Materials Research Center of National Academy of Sciences of Belarus, 220072, Minsk, Belarus.
E-mail address: vmitsiuk@gmail.com (V.I. Mitsiuk).

temperature using a PANalytical X'Pert Pro diffractometer equipped with a Cu K α radiation source ($\lambda = 1.54059$ Å) operating in a standard θ -2 θ geometry. The appropriate XRD patterns were presented in Fig. 1. The phase and structure analysis of the synthesized compositions was performed using the PANalytical X'Pert High Score Plus software with the ICDD PDF database. The lattice parameters for the analyzed solid solutions are collected in Table 1. The specific saturation magnetization and the parameters of the hysteresis loop of the specific magnetization were measured for the powder samples by the induction method on Vibrating sample magnetometer (VSM) from Cryogenic Limited. Results of these measurements, obtained in magnetic fields up to 10 T at temperatures of 4.2, 77, and 300 K are shown in Figs. 2-4, respectively.

To clarify the nature of the distribution of metal atoms over sublattices, Mössbauer studies of $Mn_{1-x}Fe_xNiGe$ ($0.05 \leq x \leq 1.00$) solid solutions were carried out. The Mössbauer experiment was performed under ordinary transmission geometry and a constant acceleration regime. $^{57m}\text{Fe}/\text{Rh}$ was used as a resonance source, the sample temperatures were $\sim 5\text{K}$, 77K (liquid nitrogen temperature) and 290K (room temperature), see Figs. 5-7. The hyperfine interactions parameters are listed in Table 2. Full width at half maximum - 0.242 ± 0.015 mm/s.

3. Results and discussion

It is known that the metalloid atoms (in our case, germanium atoms) form a hexagonally close-packed framework of the nickel arsenide structure, Fig. 8. There are two types of sites: 2a, octahedral (MeI) and 2d, trigonal-bipyramidal (MeII). These two types of structurally nonequivalent positions are filled by relatively small atoms of 3d transition metals; in our case, they are manganese, nickel, and iron. It is also known that NiAs-type structure is characterized by a high defectiveness, especially when the alloy is obtained by quenching (as in our case). Obviously, during quenching, a certain number of vacant structural positions are fixed in both sublattices. It is believed [8] that in such three-component solutions with two types of metal atoms (MnFeGe and MnNiGe), manganese atoms are localized at MeI positions, while nickel (or iron) atoms occupy only MeII positions. However, it is also known that for the structure of Ni₂In, there is a possibility of mutual “mixing” of atoms in the MeI and MeII sublattices (up to 17 at. % in MnFeGe and MnNiGe) [14].

In our case of a four-component system, the distribution of Mn, Ni, and Fe atoms over the sublattices can be judged by comparing the data of magnetic and Mössbauer studies. According to the results of the magnetic measurements, all the studied solutions exhibit magnetic interactions at nitrogen temperature (Fig. 2). However, the Mössbauer data obtained on iron atoms at nitrogen temperature do not reveal

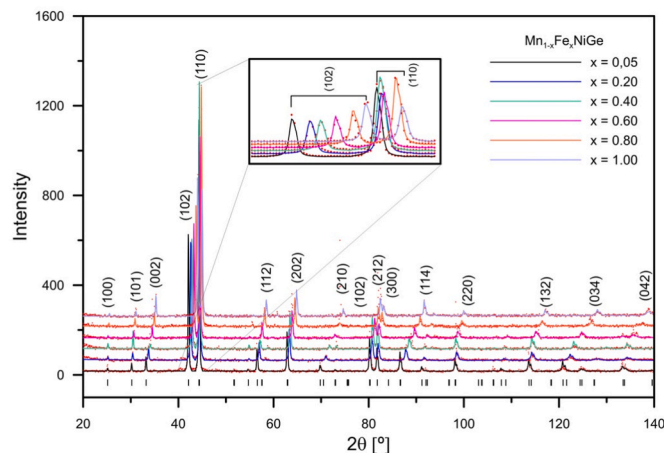


Fig. 1. XRD patterns of the $Mn_{1-x}Fe_xNiGe$ samples measured at room temperature.

Table 1

The lattice parameters of the Ni₂In type solid solutions.

x	a, nm	c, nm	c/a	$V, 10^{-2} \text{ nm}^3$
0.05	0.408(1)	0.539(1)	1.32	7.777
0.10	0.407(1)	0.536(1)	1.31	7.724
0.15	0.407(1)	0.533(1)	1.31	7.679
0.20	0.407(1)	0.530(1)	1.30	7.621
0.25	0.407(1)	0.529(1)	1.30	7.606
0.30	0.406(1)	0.527(1)	1.30	7.547
0.40	0.407(1)	0.525(1)	1.29	7.557
0.50	0.407(1)	0.521(1)	1.28	7.502
0.60	0.406(1)	0.519(1)	1.28	7.434
0.70	0.406(1)	0.516(1)	1.27	7.381
0.80	0.403(1)	0.512(1)	1.27	7.249
0.90	0.404(1)	0.510(1)	1.26	7.219
1.00	0.402(1)	0.508(1)	1.26	7.133

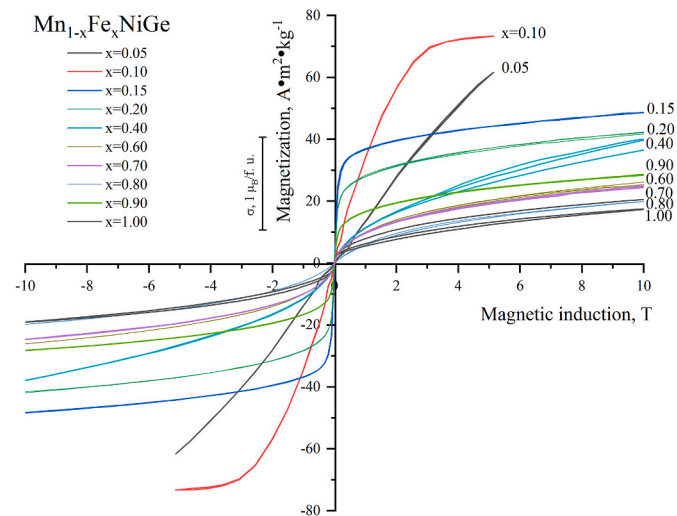


Fig. 2. Field dependences of the magnetization of $Mn_{1-x}Fe_xNiGe$ samples at 77K.

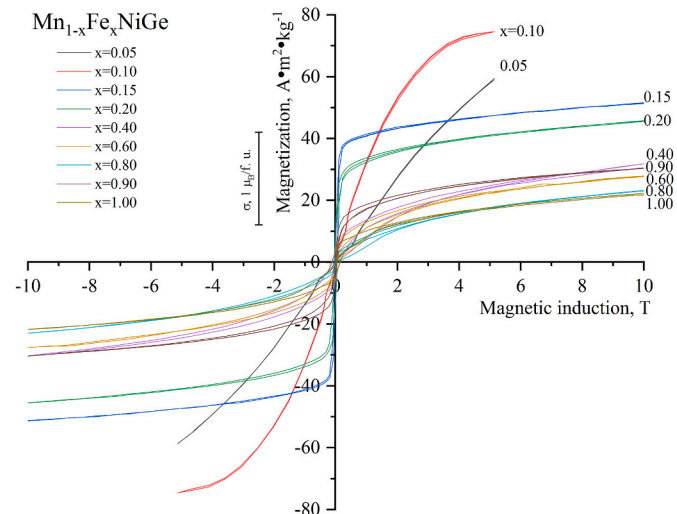


Fig. 3. Field dependences of the magnetization of $Mn_{1-x}Fe_xNiGe$ samples at 5 K.

magnetic interactions on Fe up to the iron content $x = 0.20$ (Fig. 6). This result can be explained assuming that at low iron concentrations x (up to 0.2 at.%) in the $Mn_{1-x}Fe_xNiGe$ system, Mn atoms are not replaced by iron atoms. Bearing in mind that the Mn atoms fill the octahedral sublattice MeI which determines the magnetic interactions in the alloy, and taking

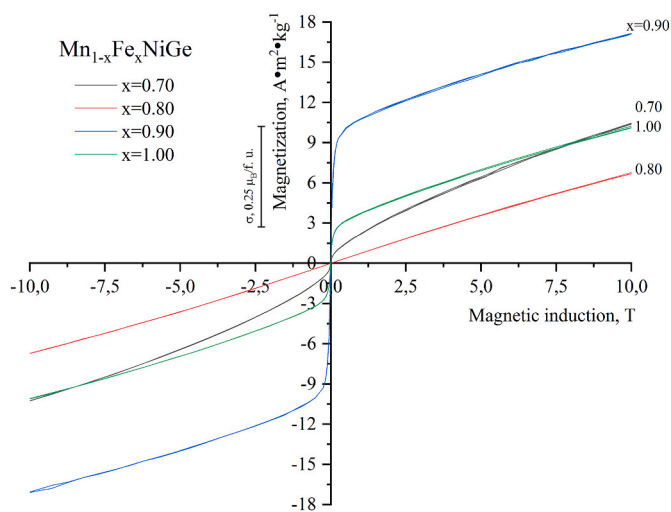


Fig. 4. Field dependences of the magnetization of $\text{Mn}_{1-x}\text{Fe}_x\text{NiGe}$ samples at room temperature.

into account that the structure is highly defective hence formation of voids in the octa sublattice is very likely, we believe that up to the $x = 0.20$ composition, iron atoms enter the sublattice of nickel atoms (MeII), while the deficiency of manganese atoms in the MeI positions is compensated by vacancies. So the magnetic hyperfine interaction of iron atoms in the Me II sublattice is blocked by the local environment of nickel atoms. This assumption is reflected in Mössbauer spectrum shape, namely, in the absence of magnetic splitting of the spectra at $T = 77\text{K}$ at such iron concentrations (see Fig. 6). This assumption is consistent with the literature data on the absence of magnetic moments on nickel atoms in the MeII sublattice [7,8]. A certain amount of magnetic iron and manganese atoms have passed into the MeII sublattice and stop the participation in the magnetic interactions, thereby somewhat reducing the overall magnetization of the alloy (see the figure for magnetic measurements for these concentrations).

A further increase in the iron content leads to the entry of Fe atoms into the manganese atoms sublattice (MeI). The Mössbauer spectra of solid solutions with $x > 0.20$ at liquid nitrogen and liquid helium temperatures (Figs. 6–7) look like magnetically split lines, which is consistent with the magnetization measurement data. The magnetic splitting of the spectra on iron in the MeI positions means the appearance of hyperfine magnetic fields on the nuclei of Fe atoms. However, the smeared shape of the spectrum indicates a wide variety of local environments of iron atoms. The imperfection of the crystal structure leads to the fact that the electric field gradient is oriented relative to the magnetization direction in more than one way, which is reflected in a significant broadening of the lines of the Mössbauer subspectra.

The magnetic and Mössbauer data obtained indicate that the iron atoms in $\text{Mn}_{1-x}\text{Fe}_x\text{NiGe}$ at concentrations up to $x \sim 0.20$ preferably fill the Me II positions replacing nickel atoms. With an increase in the iron content (at $x > 0.20$), iron replaces both the nickel atoms at MeII positions and the manganese atoms at MeI positions.

4. Conclusion

All studied $\text{Mn}_{1-x}\text{Fe}_x\text{NiGe}$ $0.05 \leq x \leq 1.00$ alloys at $T = 290\text{ K}$ are single-phase solid solutions with a hexagonal structure of the Ni_2In type. It is shown that in quaternary solid solutions $\text{Mn}_{1-x}\text{Fe}_x\text{NiGe}$ at $x < 0.20$, iron predominantly enters the sublattice of nickel atoms in MeII positions and does not participate in magnetic interactions. This fact is reflected in a magnetization decrease. As x in the $\text{Mn}_{1-x}\text{Fe}_x\text{NiGe}$ increases, iron replaces both nickel atoms in the MeII positions and manganese atoms in the MeI positions.

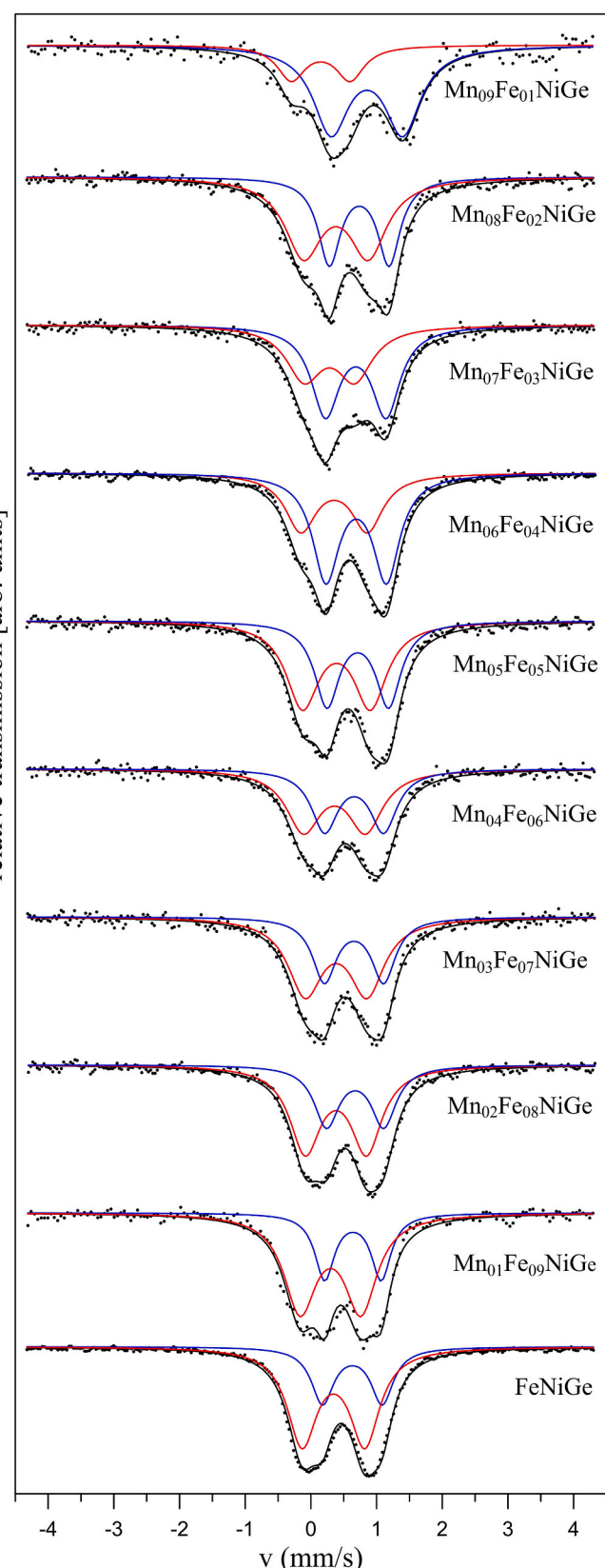
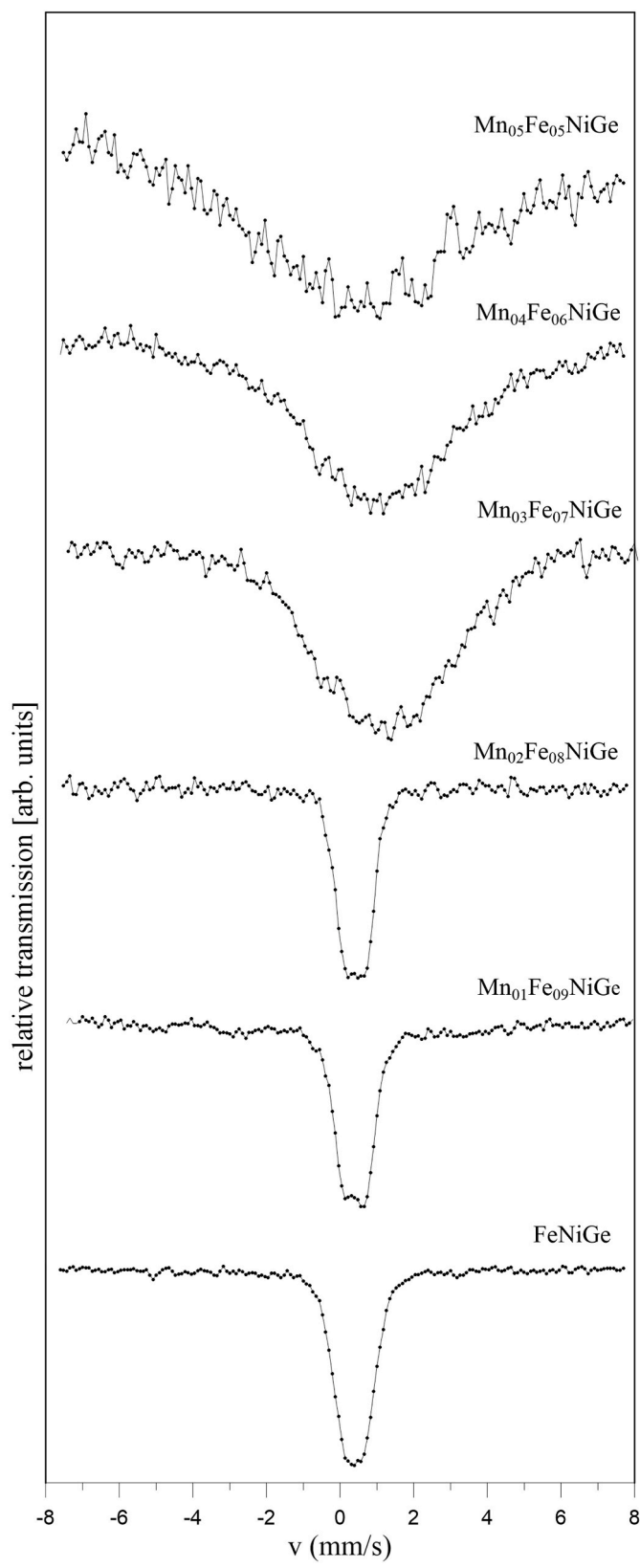
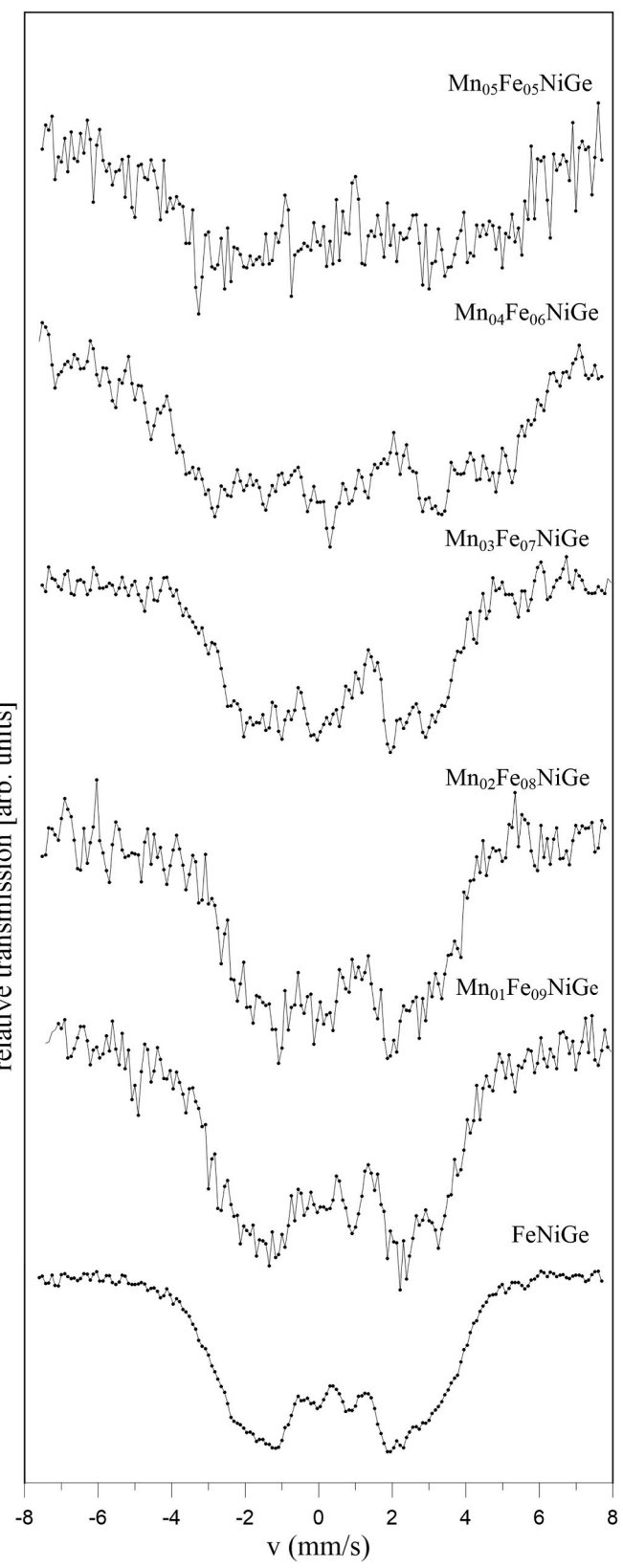


Fig. 5. Mössbauer spectra of $\text{Mn}_{1-x}\text{Fe}_x\text{NiGe}$ at room temperature.

Fig. 6. Mössbauer spectra of $\text{Mn}_{1-x}\text{FexNiGe}$ at 77 K.Fig. 7. Mössbauer spectra of $\text{Mn}_{1-x}\text{FexNiGe}$ at 4 K.

Statement of novelty

The authors affirm that the manuscript present new data which are in agreement with the aims and scope of the Journal, the text has been

approved by all the co-authors and the responsible authorities at the appropriate institutes.

Table 2

Hyperfine interactions parameters derived from room temperature Mössbauer spectra of the Ni₂In type solid solutions; IS- isomer shiftrelative to α -Fe, QS – quasrupole splitting, D – contribution, W-HFWHM, Full width at half maximum - 0.242 ± 0.015 mm/s.

sample	Subspectrum 1				Subspectrum 2			
	IS, mm/s	QS, mm/s	D %	W, mm/s	IS, mm/s	QS, mm/s	D %	W, mm/s
Mn _{0.9} Fe _{0.1} NiGe	0.242(7)	1.010(6)	37	0.57	0.950(5)	0.893(8)	63	0.33
Mn _{0.8} Fe _{0.2} NiGe	0.463(4)	0.992(4)	40	0.21	0.824(7)	0.896(5)	60	0.35
Mn _{0.7} Fe _{0.3} NiGe	0.366(4)	0.767(3)	43	0.33	0.768(5)	0.924(7)	57	0.26
Mn _{0.6} Fe _{0.4} NiGe	0.443(5)	1.007(3)	39	0.29	0.771(5)	0.921(6)	61	0.25
Mn _{0.5} Fe _{0.5} NiGe	0.468(5)	1.034(5)	57	0.30	0.798(6)	0.940(4)	43	0.23
Mn _{0.4} Fe _{0.6} NiGe	0.440(6)	0.950(3)	56	0.31	0.742(6)	0.905(5)	44	0.45
Mn _{0.3} Fe _{0.7} NiGe	0.471(6)	0.938(5)	63	0.32	0.740(5)	0.904(4)	63	0.22
Mn _{0.2} Fe _{0.8} NiGe	0.458(4)	0.933(4)	64	0.29	0.761(6)	0.8765(5)	36	0.23
Mn _{0.1} Fe _{0.9} NiGe	0.382(5)	0.927(4)	71	0.28	0.724(5)	0.863(4)	29	0.30
FeNiGe	0.433(3)	0.961(2)	69	0.28	0.708(4)	0.907(3)	31	0.21

Unit Conversion: 1 mm/s = 11.6248 MHz.

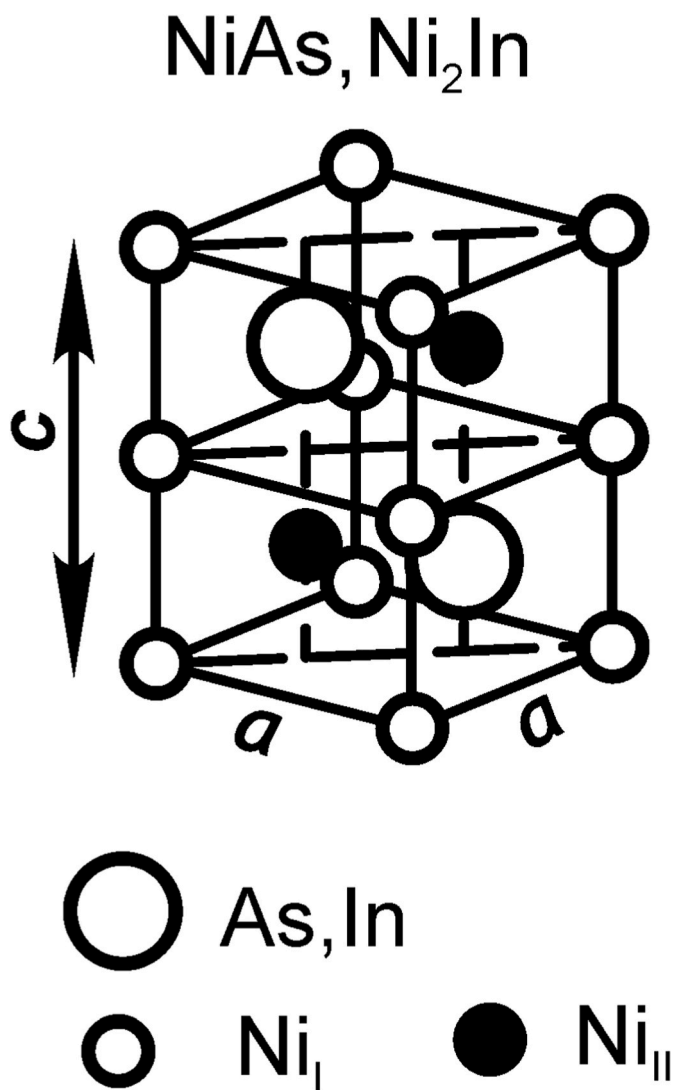


Fig. 8. Crystal structure of Ni₂In.

Declaration of competing interest

None of the authors of this paper has a financial or personal

relationship with other people or organizations that could inappropriately influence or bias the content of the paper. It is to specially state that “No Competing interests are at stake and there is No Conflict of Interest” with other people or organizations that could inappropriately influence or bias the content of the paper.

Data availability

No data was used for the research described in the article.

Acknowledgement

V.K. acknowledges the financial support from the Priority-2030 Program of NUST “MISiS” (No. K2-2022-022). The authors are grateful to G. Rimski for the sample preparation.

References

- [1] E.K. Liu, H.G. Zhang, G.Z. Xu, et al., Appl. Phys. Lett. 102 (2013), 122405, <https://doi.org/10.1063/1.4798318>.
- [2] E.H. Brück, O. Tegusi, F.R. De Boer, Material for Magnetic Refrigeration Preparation and Application, 2004, US Patent 7069729 B2.
- [3] V.I. Val'kov, V.I. Kamenev, A.V. Golovchan, et al., Phys. Solid State 63 (2021) 1889, <https://doi.org/10.1134/S1063783421050188>.
- [4] A.P. Sivachenko, V.I. Mitsuuk, V.I. Kamenev, et al., Low Temp. Phys. 39 (2013) 1051, <https://doi.org/10.1063/1.4843196>.
- [5] M. Budzynski, V.I. Val'kov, A.V. Golovchan, et al., J. Magn. Magn Mater. 396 (2015) 166, <https://doi.org/10.1016/j.jmmm.2015.08.052>.
- [6] K.A. Korolev, A.P. Sivachenko, I.F. Gribanov, et al., Chelyabinsk Physical and Mathematical Journal 5 (2020) 569, <https://doi.org/10.47475/2500-0101-2020-15416>.
- [7] E. Liu, W. Wang, L. Feng, et al., Nat. Commun. 3 (2012) 873, <https://doi.org/10.1038/ncomms1868>.
- [8] A. Szytula, A.T. Pędziwi, Z. Tomkowicz, et al., J. Magn. Magn Mater. 25 (1981) 176, [https://doi.org/10.1016/0304-8853\(81\)90116-5](https://doi.org/10.1016/0304-8853(81)90116-5).
- [9] M.R.L.N. Murthy, M.G. Natera, R.J. Begum, et al., Proc. Nucl. Phys. And Solid State Physics, Symp. Bombay, 1972, p. 513.
- [10] Z. Cheng-Liang, W. Dun-Hui, C. Jian, et al., Chin. Phys. B 20 (2011), <https://doi.org/10.1088/1674-1056/20/9/097501>, 097501-1.
- [11] C. Zhang, D. Wang, Q. Cao, et al., J. Phys. D Appl. Phys. 43 (2010), 205003, <https://doi.org/10.1088/0022-3727/43/20/205003>.
- [12] A.D. Bruce, R.A. Cowley, Structural Phase Transitions, Taylor and Francis, 1981, p. 326.
- [13] J. Łażewski, P. Piekarz, K. Parlinski, Phys. Rev. B 83 (2011), <https://doi.org/10.1103/PhysRevB.83.054108>, 054108-1.
- [14] M. Budzynski, V.I. Valkov, A.V. Golovchan, et al., Nukleonika 60 (2015) 11, <https://doi.org/10.1515/nuka-2015-0031>.